Enhance WLEDs Performance with Additional Phosphor Materials in Multi-Layer Remote Structure

Nguyen Hai Son DANG[1], *Doan Minh Thong NGUYEN*[1], *Thi Phuong Loan NGUYEN*[1], *Doan Quoc Anh NGUYEN*[2,*], *Hsiao-Yi LEE*[3]

[1]Faculty of Electrical and Electronics Engineering, Ton Duc Thang University, Ho Chi Minh City, Vietnam
[2]Power System Optimization Research Group, Faculty of Electrical and Electronics Engineering, Ton Duc Thang University, Ho Chi Minh City, Vietnam
[3]Department of Electrical Engineering, National Kaohsiung University of Science and Technology, Kaohsiung, Taiwan

*Corresponding Author: Doan Quoc Anh NGUYEN (Email: nguyendoanquocanh@tdtu.edu.vn)
(Received: 14-Oct-2020; accepted: 15-Jul-2021; published: 30-Sep-2021)
DOI: http://dx.doi.org/10.55579/jaec.202153.305

Abstract. *One of the most important factors used to evaluate lighting performances of WLEDs is the angular color uniformity (ACU). The triple-layer remote phosphor structure is considered as a proposed mechanism for elevating the ACU of a WLED. The analysis on the triple-layer structure's efficiency is specifically demonstrated in this article. Additionally, there are detailed comparisons between the triple-layer (TL) and the dual-layer (DL) geometries to reinforce the idea of using TL packaging for WLED optical enhancements. The WLEDs with average correlated color temperatures (ACCTs) of 6600 K and 7700 K are utilized for experiments. According to the outcomes, the attained color rendering index from DL design is higher than the one from TL package. However, the TL shows better color quality scale (CQS) than the DL, regardless of ACCTs. Besides, not only does the TL yield better CQS but also heighten the lumen efficiency. On top of that, the ACU of TL WLED model is much higher than that of the DL as a result of deviated correlated color temperature reduction at all ACCTs. This result is more obvious at the high ACCT of 7700 K, in other words, the ACU of a high-ACCT WLED shows more visible enhancement with TL structure. From these results, the triple-layer remote phosphor structure stands out as the promising advancement in the production of high-quality WLEDs.*

Keywords

Dual-layer phosphor, triple-layer phosphor, Mie-scattering theory, luminous efficacy, color rendering index.

1. Introduction

With outstanding features, including small size, energy efficiency, eco friendliness, and longevity, which have gained much recognition in the lighting industry, white light-emitting diodes (WLEDs) have spread out in illuminating applications. Lighting design, street lighting, household lighting, and headlamps are the aspects that WLEDs are frequently utilized [1]-[3]. In general, the popular method for phosphor-converted WLED production is inte-

grating blue LED chips with organic resin/yellow $Y_3Al_5O_{12}:Ce^{3+}$ ($YAG:Ce^{3+}$) phosphor composition [4, 5]. Despite its popularity, the organic encapsulation is an obstacle for the development of high-power WLED devices. As the organic silicone encapsulant is inferior in temperature stability and photonic terms, it easily decays and becomes yellowish. As a result, there are degradations in lumen efficiency (LE) and long-term reliability, together with the occurrence of color shift in WLED devices after a long service time [6, 7]. Besides that, the organic resin has a lower refractive index (RI) which is approximately 1.5, compared to the RI value of the yellow phosphor $YAG:Ce^{3+}$ (about 1.83). This difference in RIs causes the lights to be reflected and finally absorbed in a large portion, which means the amount of light that can escape the package is reduced [8, 9].

A phosphor-in-glass (PiG) structure, fabricated by sintering glass powders and phosphor grains at a temperature under 800^0C, was proposed to settle the problems of organic silicone encapsulation. The reason making PiG a better choice for WLED manufacture is their impressive characteristics, which includes the high durability and temperature stability, and low coefficient of thermal expansion [10]-[12]. The presence of glass powders adds more ions of large polarizability to the PiG's structure, raising the RI of PiG converter. Recently, a PiG converter with $YAG:Ce^{3+}$ yellow phosphor base has been fabricated by using the techniques of screen-printing and low-temperature sintering to combine $YAG:Ce^{3+}$ phosphor with borosilicate glass. This $YAG:Ce^{3+}$ based PiG converter can result in cool white lights accompanied by a 114 lm/W lumen output efficiency, a 5524 K color temperature, and a 69 CRI (color rendering index) [13, 14]. As can be seen from the obtained figures, it is hard for $YAG:Ce^{3+}$ PiG to generate natural white lights and improve CRI value at the same time owing to the lack of red-light components in its emitted white lights. So, the $CaAlSiN_3:Eu^{2+}$ ($CASN:Eu^{2+}$) red phosphors were integrated into the glass matrix to improve the CRI of PiG based WLEDs [15]-[17]. However, there were the thermal reduction occurring to the red phosphor particles in the co-sintering time and the interfacial reaction between the red phosphor and the glass powder. These occurrences were the main cause of the red-phosphor quantum efficiency degradation [18, 19]. Moreover, the total internal reflection (TIR) at the contacting surface between the glass matrix and the air existed in WLEDs with the flat PiG converter due to the discrepancy between the glass and air refractive indices, which trapped light and reduced WLED lighting capacity. Meanwhile, the structure with micro/nano patterns was recognized as an effective method to reduce the TIR as well as promote the efficiency in light extraction. For that reason, researchers proposed various directions to produce patterned structures, some of which were lithography, photoresist reflow, direct laser writing, and inkjet imprinting. Yet, the problem here was that the photolithographic stage included in the production process of most methods cost too much and took a lot of time to be carried out and also resulted in environmental defilement. For the direct laser writing technique, the patterned configurations can be produced precisely but it was high-cost and inadequate for large-scale production. The inkjet printing was unfavorable in WLED fabrication due to its inhomogeneous morphology and large size in spite of its mask-less, large-scale, and low-cost manufacturing features. Hence, figuring out a strategy that can flexibly and effectively promote light extraction and color uniformity for $YAG:Ce^{3+}$ PiG is one of the most challenging issues for WLED manufacturers.

In order to suggest a potential phosphor structure for $YAG:Ce^{3+}$ PiG to achieve better performances, the triple-layer remote phosphor configuration is introduced in this research paper. The studied remote phosphor structure consists of three different phosphor films which are red phosphor $LaAl_3B_4O_{12}:Eu^{3+}$, green phosphor $LiAlO_2:Mn^{2+}$, and yellow phosphor $YAG:Ce^{3+}$. The preset correlated color temperatures of the WLED models are 6600 K and 7700 K. Additionally, in this study, the WLED model of dual-layer structure with the red phosphor layer is fabricated, besides the proposed triple-layer configuration. The utilization of these two different phosphor structures is to analyze and compare the optical performances of WLED packages with each structure for the verification of

triple-layer structure's efficiency. Moreover, the Mie-scattering and the Lambert-Beer law are applied to calculate and examine the scattering ability and the light power of the WLED using two multi-layer remote phosphor structures [20]. The results generally show that the triple-layer configuration is better than the dual-layer one in terms of the uniformity of color distribution and luminescence. The presence of the red and green phosphor films is beneficial to the optical properties of the WLEDs. Particularly, the red phosphor $LaAl_3B_4O_{12}:Eu^{3+}$ layer can boost the red-light components to enhance the color rendering ability, while the green $LiAlO_2:Mn^{2+}$ film helps to improve the light extraction efficiency. Therefore, the triple-layer performs higher lighting efficiency than the dual-layer. Hence, the triple-layer is believed to be the suitable alternative to the dual-layer structure.

The organization for the rest of this article can be described as follows. The fabrications of the yellow, green and red phosphors as well as the organization of the phosphor layers are included in Section 2. Next, Section 3 presents the mathematic model for the analysis of phosphor layers' optical performance, followed by detailed discussions on the obtained outcomes. Finally, Section 4 summarizes the results and suggestions in the whole research for reference.

2. Research method

2.1. Preparation of phosphor materials

This part demonstrates the preparation processes and optical properties of green $LiAlO_2:Mn^{2+}$, red $LaAl_3B_4O_{12}:Eu^{3+}$ and yellow $Y_3Al_5O_{12}:Ce^{3+}$ phosphor particles. The composition of each phosphor material is presented in Tabs. 1, 2 and 3.

The fabrication of the green phosphor $LiAlO_2:Mn^{2+}$ includes two stages of firing but at first all the ingredients must be slurried in methanol to create the fundamental mixture. Then, let the mixture dry naturally in air. The first stage of firing is carried out after the dried mixture is turned into powder. In this stage, the powder is fired at 1200^0C in covered alumina crucibles with a N_2 flow for an hour. As soon as the firing time is finished, the product is taken out for powederizing. In the next stage, the powder goes through another 2-hour firing process in open quartz boats filled with CO flows at a higher temperature of 1250^0C. The attained green phosphor $LiAlO_2:Mn^{2+}$ has an emission peak of 2.375 eV, an emission width of 0.15 eV, approximate 6–8% excitation efficiency by e-beam, and non-exponetial decay with long and strong phosphorescence.

Tab. 1: The composition of green phosphor LiAlO2:Mn^{2+}.

Ingredients	Mole %	By weight
Li_2CO_3	99 (of Li)	36.6
Al_2O_3	499 (of Al)	254
$MnCO_3$	2	2.3

Tab. 2: The composition of red phosphor $LaAl_3B_4O_12:Eu^{3+}$.

Ingredients	Mole %	By weight
La_2O_3	90 (of La)	147
Eu_2O_3	10 (of Eu)	17.6
Al_2O_3	300 (of Al)	153
H_3BO_3	410	254

Tab. 3: The composition of yellow phosphor $Y_3Al_5O_{12}:Ce^{3+}$.

Ingredients	Mole %	By weight
Y_2O_3	100	10
Al_2O_3	200	9.03
$Ce(NO_3)_3 \cdot 4H_2O$	2	0.555
B_2O_3	2	0.062

For the red phosphor $LaAl_3B_4O_{12}:Eu^{3+}$ preparation, the process starts with dry milling or milling to mix all the ingredients. After that, the mixture is fried for three times in open quartz boats with air. In the first firing, it is carried out at around 500^0C and finished with the composition being powderized. The second firing process occurs at 900^0C within 1 hour and is also followed by the powderizing. The final firing stage is a 2-hour process at 1200^0C. After the third firing stage is finished, the red phosphor $LaAl_3B_4O_{12}:Eu^{3+}$ is

obtained with the following optical characteristics: 2.005 eV and 2.020 eV emission peaks and excitation efficiency by UV at +(4.88 eV), -(3.40 eV) photon energy.

The process of preparing yellow phosphor $Y_3Al_5O_{12}$:Ce^{3+} includes 2 stages of firing, and can be demonstrated as follows. The listed ingredients of yellow phosphor composition are mixed together by dry grinding in a mortar for 30 minutes. After that, this mixture is pressed into pellets with a hydraulic press machine at 40,000 psi. The pressed mixture is then dried in air and powderized before being fired. The first firing is conducted afterwards with N_2 flows, at the temperature of 1000^0C for 2 hours. As soon as the firing finishes, the product is taken out and turned into powders. Subsequently, the powder is re-pressed into pellets. The pellets are next fired in the combination of 95% N_2 +5% H_2 for 3 hours and at 1400^0C. The attained $Y_3Al_5O_{12}$:Ce^{3+} phosphor has the violet emission color, 528-nm emission peak, and emission width of 4580 cm^{-1}.

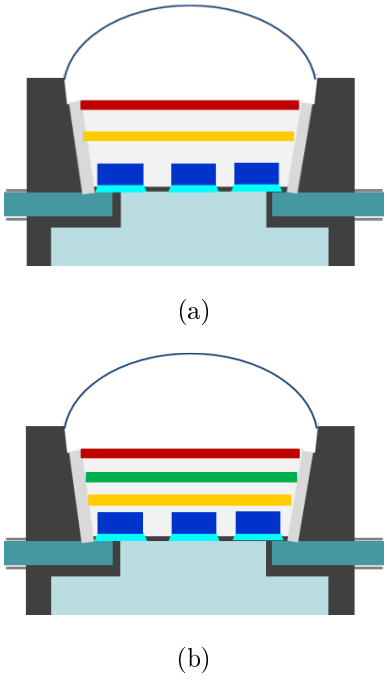

Fig. 1: Illustrations of multi-layer phosphor structures of white LEDs: (a) Dual-layer phosphor (DL) and (b) triple-layer phosphor (TL).

2.2. Simulation process

The illustrations in Fig. 1 show the configurations of dual-layer (Fig. 1(a)), and triple-layer (Fig. 1(b)) remote phosphor used in this study. In the dual-layer model, the red phosphor layer is above the yellow phosphor YAG:Ce^{3+} which covers the blue chip area. Meanwhile, in the triple-layer one, the green phosphor film is placed between the yellow and the red phosphor layers. Besides that, the substrate where the blue LED chips are attached is made of aluminum nitride, the average correlated color temperatures (ACCTs) applied for these WLEDs models are 6600 K and 7700 K, and the thickness of each phosphor layer is set at 0.08 mm. For the stability of the ACCTs, YAG:Ce^{3+} yellow phosphor concentration varies in accordance with the changes of red or green phosphor concentrations. Moreover, in both DL and TL structures, the YAG:Ce^{3+} concentrations are various at each ACCT, which enriches the scattering ability inside the LED package and results in the diversity in device's optical performances.

Figure 2 presents that the TL structure has lower concentration of YAG:Ce^{3+} than the DL structure does, at any ACCT. Given that both structures have the same ACCTs, the higher concentration of YAG:Ce^{3+} implies the higher chance of backscattering occurrences, and this results in the degradation of lumen efficiency. In addition to that, the rising YAG:Ce^{3+} concentration also causes the imbalance to the white light color components (red, yellow, and green) and thus reducing the chromatic homogeneity of the WLED. In other words, the heightened YAG:Ce^{3+} concentration probably diminishes either luminous efficacy or color quality of WLED devices.

To achieve the advancement in lumen output and color uniformity for WLED packages with remote phosphor structures, the backscattering must be minimized with the enhancement in red light components. In addition to the red lights, the green lights play an important role in managing the quality of chromaticity and luminous flux. Thus, it has turned out that the triple-layer remote phosphor configuration can become

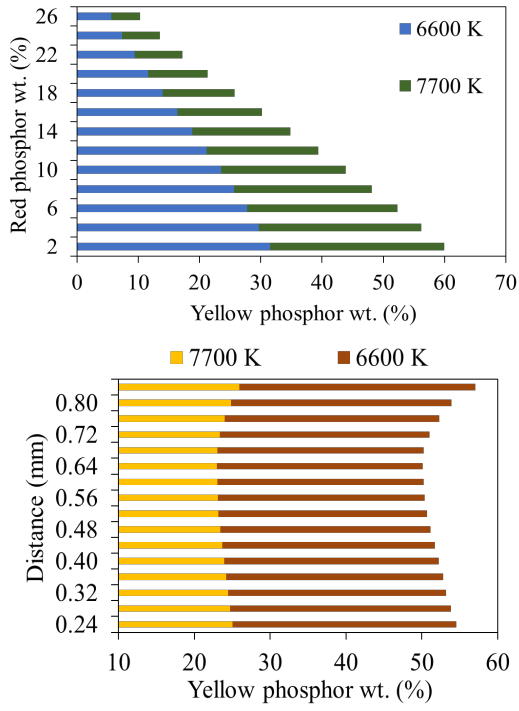

Fig. 2: The concentration of yellow YAG:Ce^{3+} phosphor in each remote phosphor structure at each different ACCT: (top) DL; (bottom) TL.

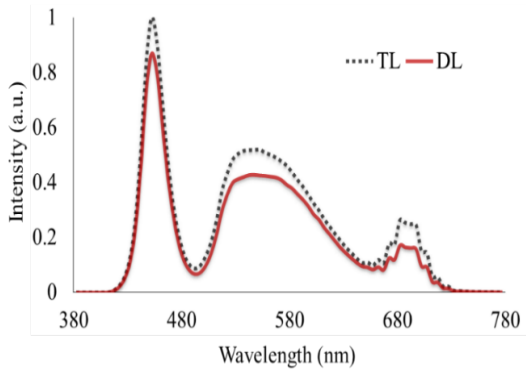

Fig. 3: Emission spectra of phosphor configurations.

one of the most flexible and effective solutions. Hence, this article will provide more vital results of using TL structures through comparison and spectral emission results to reinforce this statement.

3. Results and analysis

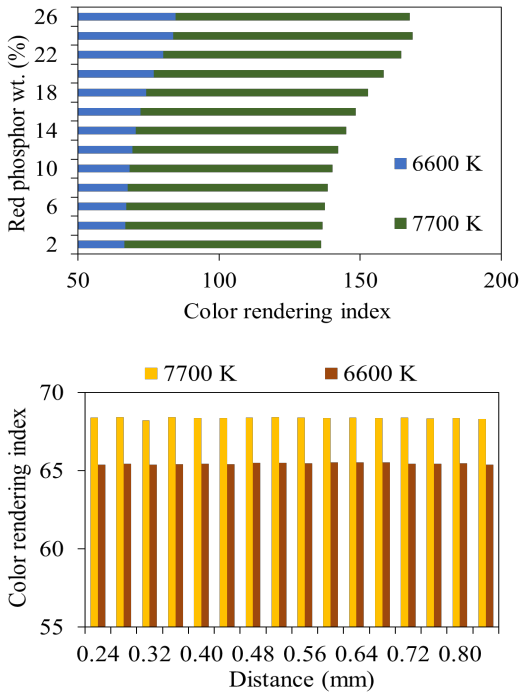

Fig. 4: The concentration of yellow YAG:Ce^{3+} phosphor in each remote phosphor structure at each different ACCT: (top) DL; (bottom) TL.

The comparison between the DL and TL structures in terms of CRI is demonstrated in Fig. 4. As can be seen, DL structure yields better CRI than TL structure at all ACCTs. Additionally, the CRI tends to go upward along with the increase of red phosphor concentration and shows considerable improvement at the high ACCT of 7700 K. The $LaAl_3B_4O_{12}$:Eu^{3+} red phosphor layer in this DL structure benefits the CRI as it increases the red photons in light components. Managing CRI in WLED with high ACCT (more than 7000 K) is still a complicated and difficult task, which emphasizes the importance of this information to WLED manufacturers. Meanwhile, in the case of TL structure, CRI seems to be stable at all ACCTs. Thus, if the goal of the manufacturer is attaining high-CRI WLEDs, the DL structure can be chosen. On the other hand, the CRI is an essential parameter used to examine the WLED color quality;

however, it cannot fully evaluate all aspects of a light source. According to many researchers in the recent years, color quality scale (CQS) is considered as a more thorough index in evaluating the chromaticity of white lights. The reason is that CQS includes three different factors for color examination: color rendering index, the preference of viewers, and the chromaticity coordinate. The results of CQS in DL and TL packages are illustrated in Fig. 5, from which a general comparison is drawn. In contrast to the CRI results, the CQS in TL structure is much better than that in the DL. This can be attributed to the ability of balancing the red, yellow, and green light colors in the WLED of the triple-layer remote phosphor structure.

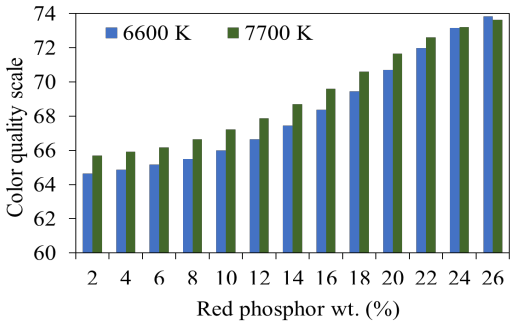

Fig. 5: Color quality scale of phosphor configurations corresponding to ACCTs.

According to the discussion above, the TL structure can be applied to mass-production when the manufacturer aims to accomplish high color quality for WLEDs. However, this finding has raised a doubt about if the luminous flux could maintain the same performance when color quality is enhanced. The comparison between the luminous output of the DL and of the TL is necessary to solve this question. This paper uses a mathematic system to verify the advancement in the lighting efficiency of these structures. In particular, the equations used to calculate the transmitted blue light and converted yellow light in both remote phosphor structures are demonstrated and the results are explained and discussed afterwards.

In the case of DL model having h thickness for each phosphor layer, its transmitted blue light and converted yellow light are:

$$PB_2 = PB_0 e^{-\alpha_{B_2} h} e^{-\alpha_{B_2} h} = PB_0 e^{-2\alpha_{B_2} h} \quad (1)$$

$$\begin{aligned} PY_2 &= \frac{1}{2}\frac{\beta_2 PB_0}{\alpha_{B_2} - \alpha_{Y_2}} \left[e^{-\alpha_{Y_2} h} - e^{-\alpha_{B_2} h}\right] e^{-\alpha_{Y_2} h} \\ &+ \frac{1}{2}\frac{\beta_2 PB_0}{\alpha_{B_2} - \alpha_{Y_2}} \left[e^{-\alpha_{Y_2} h} - e^{-\alpha_{B_2} h}\right] \\ &= \frac{1}{2}\frac{\beta_2 PB_0}{\alpha_{B_2} - \alpha_{Y_2}} \left[e^{-2\alpha_{Y_1} h} - e^{-2\alpha_{B_1} h}\right] \end{aligned} \quad (2)$$

Meanwhile, for the TL configuration, each phosphor film has a thickness of $\frac{2h}{3}$ and computations of its transmitted blue light and converted yellow light can be demonstrated as:

$$\begin{aligned} PB_3 &= PB_0 e^{-\alpha_{B_2}\frac{2h}{3}} e^{-\alpha_{B_2}\frac{2h}{3}} e^{-\alpha_{B_2}\frac{2h}{3}} \\ &= PB_0 e^{-2\alpha_{B_3} h} \end{aligned} \quad (3)$$

$$\begin{aligned} PY_3' &= \frac{1}{2}\frac{\beta_3 PB_0 e^{-\alpha_{Y_3}\frac{2h}{3}}}{\alpha_{B_3} - \alpha_{Y_3}} \left[e^{-\alpha_{Y_3}\frac{2h}{3}} - e^{-\alpha_{B_3}\frac{2h}{3}}\right] \\ &+ \frac{1}{2}\frac{\beta_3 PB_0 e^{-\alpha_{B_3}\frac{2h}{3}}}{\alpha_{B_3} - \alpha_{Y_3}} \left[e^{-\alpha_{Y_3}\frac{2h}{3}} - e^{-\alpha_{B_3}\frac{2h}{3}}\right] \\ &= \frac{1}{2}\frac{\beta_3 PB_0}{\alpha_{B_3} - \alpha_{Y_3}} \left[e^{-\alpha_{Y_3}\frac{4h}{3}} - e^{-2\alpha_{B_3}\frac{4h}{3}}\right] \end{aligned} \quad (4)$$

$$\begin{aligned} PY_3 &= PY_3' e^{-\alpha_{Y_3}\frac{2h}{3}} \\ &+ \frac{1}{2}\frac{\beta_3 PB_0 e^{-2\alpha_{B_3}\frac{4h}{3}}}{\alpha_{B_3} - \alpha_{Y_3}} \left[e^{-\alpha_{Y_3}\frac{2h}{3}} - e^{-\alpha_{B_3}\frac{2h}{3}}\right] \\ &= \frac{1}{2}\frac{\beta_3 PB_0 e^{-\alpha_{Y_3}\frac{2h}{3}}}{\alpha_{B_3} - \alpha_{Y_3}} \left[e^{-\alpha_{Y_3}\frac{4h}{3}} - e^{-\alpha_{B_3}\frac{4h}{3}}\right] \\ &+ \frac{1}{2}\frac{\beta_3 PB_0 e^{-\alpha_{B_3}\frac{4h}{3}}}{\alpha_{B_3} - \alpha_{Y_3}} \left[e^{-\alpha_{Y_3}\frac{2h}{3}} - e^{-\alpha_{B_3}\frac{2h}{3}}\right] \\ &= \frac{1}{2}\frac{\beta_3 PB_0}{\alpha_{B_3} - \alpha_{Y_3}} \left[e^{-\alpha_{Y_3} h} - e^{-2\alpha_{B_3} h}\right] \end{aligned} \quad (5)$$

h in the above equations indicates the thickness of each phosphor film in the remote phosphor packages. Besides that, the subscripts "2" and "3" present the DL and TL structures, respectively. β shows the conversion coefficient for blue light converting to yellow light, and γ means the reflection coefficient of the yellow light. PB_0 demonstrates the intensities of blue light (PB) and yellow light (PY) which are the light intensity from blue LED. α_B; α_Y describes

the fractions of the energy loss of blue and yellow lights during their propagation in the phosphor layer, respectively. In addition, PY'_3 in Eq. (4) is the parameter indicating the yellow light transmitted through two phosphor films.

The lighting performance of a WLED device is significantly enhanced with the application of the triple-layer remote phosphor structure, which is even higher than the light output of the dual-layer model:

$$\frac{(PB_3 - PY_3) - (PB_2 + PY_2)}{PB_2 + PY_2} > \frac{e^{-2\alpha_{B_3}h} - e^{-2\alpha_{B_2}h}}{e^{-2\alpha_{Y_3}h} - e^{-2\alpha_{B_2}h}} > 0 \qquad (6)$$

The scattering properties of phosphor layers are studied through Mie-scattering theory [21], by which the computation of scattering cross section C_{sca} for spherical particles is carried out. The Lambert-Beer law is also utilized for the calculation of light power:

$$I = I_0 \exp(-\mu_{\text{ext}} L) \qquad (7)$$

In Eq. (7), the incident light power is indicated by I_0, while L (mm) expresses the thickness of the phosphor film. The extinction coefficient μ_{ext} is calculated through the following equation: $\mu_{\text{ext}} = N_r C_{\text{ext}}$, with the parameters of N_r (mm^{-3}) and C_{ext} (mm^2) are the number density distribution and the extinction cross-section of phosphor particles, respectively. As the Eq. (6) implied, the lumen efficiency of applying the triple-layer remote phosphor structure is higher than that of using the dual-layer package. In Fig. 6, the graphs also present clearly that the luminous flux emitted from the TL model is better than the DL. The explanation for this result is the developed emission intensity in the wavelength from 500–600 nm of the triple-layer phosphor as a result of YAG:Ce^{3+} concentration decreased to stabilize the ACCT. Therefore, the amount of backscattering lights inside the triple-layer remote phosphor WLED packages is minimized, allowing the LED chip's blue lights to be easily transmitted through the YAG:Ce^{3+} phosphor layer to other phosphor films. It can be said that the TL contributes greatly to a more effective conversion of the blue light energy from the blue chips, so in comparison with the dual-layer package, the triple-layer model can generate greater intensity in white-light emission spectrum, resulting in the superior luminescence. Thus, the assumption about that the TL structure can yield higher lumen output and more homogeneous color for white lights has been proved, which also proves that optical performances including CQS and LE can be enhanced with TL structure.

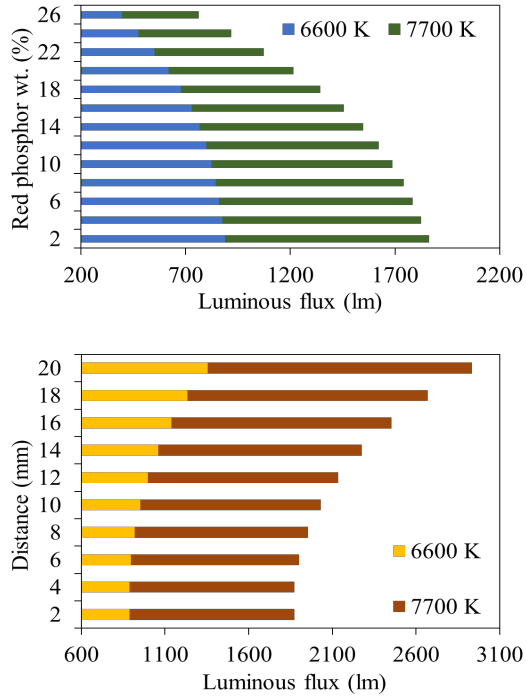

Fig. 6: Luminous output (LO) of phosphor configurations corresponding to ACCTs: (top) DL; (bottom) TL.

Besides the lumen output, the chromaticity of the white light is also an important factor of a high-quality WLED. Therefore, in many studies, various methods are proposed with the aim of enhancing the color uniformity of the white light, for example, using scattering enhancement nano particles (SiO_2, $CaCO_3$,...), or fabricating conformal phosphor configuration. It was recorded that chromatic homogeneity enhanced with these techniques but the luminous flux declined. On the other hand, the discussion above has confirmed that the triple-layer remote phosphor structure can ben-

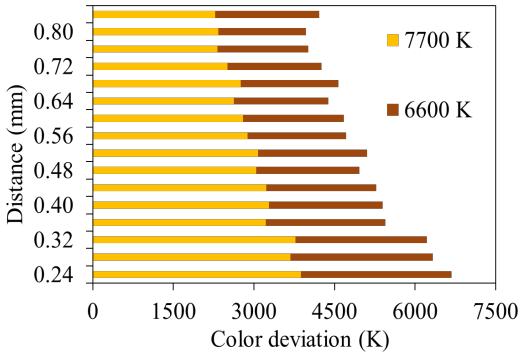

Fig. 7: Correlated color temperature deviation (D-CCT) of remote phosphor configurations corresponding to ACCTs.

efit both of these optical properties for WLEDs. The addition of two phosphor layers, red phosphor $LaAl_3B_4O_{12}:Eu^{3+}$ and green phosphor $LiAlO_2:Mn^{2+}$, increases the scattering properties of lights, the green and red light components, to balance the color elements, resulting in a more uniform chromaticity of white lights. Moreover, the remote phosphor packaging contributes significantly to backscattering reduction in WLEDs, and as a result the lumen output is better. However, to elevate the power transmission to the highest, the phosphor concentrations must be adjusted properly, according to Eq. (7) that based on the Beer's law. Figure 7 is the demonstration of the correlated color temperature deviation (D-CCT) from the remote phosphor configurations. Obviously, the TL structure is more beneficial to the color uniformity than the DL structures.

The D-CCT of the TL is greatly reduced especially at high ACCT WLEDs above 7700 K. The lower D-CCT leads to the better chromatic homogeneity since the scattering events inside the WLED packages are enhanced by the phosphor layers. The increase in the internal scattering however seems to decrease the luminous flux but it is acceptable as the benefit of backscattering reduction from TL is enough to compensate lumen decrease. Hence, we can assure that the improvement in both color quality and lumen efficiency can be achieved with the TL structure.

4. Conclusions

The effects of the dual-layer and triple-layer remote phosphor structures on the lighting properties of WLEDs with 6600 K and 7700 K ACCTs are described and compared in this research paper. The phosphor components of the remote phosphor models are red phosphor $LaAl_3B_4O_{12}:Eu^{3+}$, green phosphor $LiAlO_2:Mn^{2+}$, and yellow phosphor $YAG:Ce^{3+}$. The results of experiments are examined with the Mie-scattering theory and the Beer's law. The outcomes demonstrate that the TL structure is more advantageous in improving the color quality and the luminous efficiency of the WLED than the DL configuration. All these enhancements can be attributed to the presence of both green and red phosphor layers in the packaging structure. The green phosphor $LiAlO_2:Mn^{2+}$ adds more green photons for better color uniformity and emitted flux. Meanwhile, the red phosphor $LaAl_3B_4O_{12}:Eu^{3+}$ increases the red lights to improve the CRI and CQS of white light. Though the TL is inferior in the CRI but its CQS is much better, compared to those of the DL structure. Moreover, the color uniformity depends on the balance of three colors (yellow, green, and red), so the triple-layer becomes the more suitable structure for WLEDs to achieve this goal. In addition to that, the TL results in a significant decrease in backscattering light, which increases the lumen output even higher than the one in the DL. In short, the TL can be simultaneously better the chromaticity and the luminescence for WLED. With the information provided in this article, manufacturers can decide the remote phosphor package that matches their requirements for WLED production.

References

[1] Talone, M., & Zibordi, G. (2020). Spatial uniformity of the spectral radiance by white LED-based flat-fields. *OSA Continuum, 3*(9), 2501-2511.

[2] Zhong, W., Liu, J., Hua, D., Guo, S., Yan, K., & Zhang, C. (2019). White

LED light source radar system for multi-wavelength remote sensing measurement of atmospheric aerosols. *Applied optics, 58*(31), 8542-8548.

[3] Kim, J. O., Jo, H. S., & Ryu, U. C. (2020). Improving CRI and Scotopic-to-Photopic Ratio Simultaneously by Spectral Combinations of CCT-tunable LED Lighting Composed of Multi-chip LEDs. *Current Optics and Photonics, 4*(3), 247-252.

[4] Zhou, Y., Wei, Y., Hu, F., Hu, J., Zhao, Y., Zhang, J., ... & Chi, N. (2020). Comparison of nonlinear equalizers for high-speed visible light communication utilizing silicon substrate phosphorescent white LED. *Optics express, 28*(2), 2302-2316.

[5] Anh, N. D. Q., Le, P. X., & Lee, H. Y. (2019). Selection of a remote phosphor configuration to enhance the color quality of white LEDs. *Current Optics and Photonics, 3*(1), 78-85.

[6] Guo, Q., Li, M., Yue, K., Yan, Y., Xie, F., Zhang, C., ... & Peng, G. D. (2021). Characterization of YAG: Ce phosphor dosimeter by the co-precipitation method for radiotherapy. *Applied Optics, 60*(11), 3044-3048.

[7] Yuce, H., Guner, T., Balci, S., & Demir, M. M. (2019). Phosphor-based white LED by various glassy particles: control over luminous efficiency. *Optics letters, 44*(3), 479-482.

[8] Yang, L., Zhang, Q., Li, F., Xie, A., Mao, L., & Ma, J. (2019). Thermally stable lead-free phosphor in glass enhancement performance of light emitting diodes application. *Applied optics, 58*(15), 4099-4104.

[9] Nahavandi, A. M., Safi, M., Ojaghi, P., & Hardeberg, J. Y. (2020). LED primary selection algorithms for simulation of CIE standard illuminants. *Optics Express, 28*(23), 34390-34405.

[10] Su, V. C., & Gao, C. C. (2020). Remote GaN metalens applied to white light-emitting diodes. Optics Express, 28(26), 38883-38891.

[11] Chen, F. B., Chi, K. L., Yen, W. Y., Sheu, J. K., Lee, M. L., & Shi, J. W. (2019). Investigation on modulation speed of photon-recycling white light-emitting diodes with vertical-conduction structure. *Journal of Lightwave Technology, 37*(4), 1225-1230.

[12] Xu, S., Hu, H., Shi, Q., Yang, B., Zhao, L., Wang, Q., & Wang, W. (2021). Exploration of yellow-emitting phosphors for white LEDs from natural resources. *Applied Optics, 60*(16), 4716-4722.

[13] Keshri, S., Marín-Sáez, J., Naydenova, I., Murphy, K., Atencia, J., Chemisana, D., ... & Martin, S. (2020). Stacked volume holographic gratings for extending the operational wavelength range in LED and solar applications. *Applied optics, 59*(8), 2569-2579.

[14] Xi, X., Zhang, L., Kang, J., Li, Y., Wang, Z., Fei, B., ... & Chen, H. (2021). Chip-level Ce: GdYAG ceramic phosphors with excellent chromaticity parameters for high-brightness white LED device. *Optics Express, 29*(8), 11938-11946.

[15] El-Ghoroury, H. S., Nakajima, Y., Yeh, M., Liang, E., Chuang, C. L., & Chen, J. C. (2020). Color temperature tunable white light based on monolithic color-tunable light emitting diodes. *Optics express, 28*(2), 1206-1215.

[16] Zhu, P., Zhu, H., Adhikari, G. C., & Thapa, S. (2019). Spectral optimization of white light from hybrid metal halide perovskites. *OSA Continuum, 2*(6), 1880-1888.

[17] Xu, Q., Meng, L., & Wang, X. (2019). Nanocrystal-filled polymer for improving angular color uniformity of phosphor-converted white LEDs. *Applied optics, 58*(27), 7649-7654.

[18] Zhang, G., Ding, K., He, G., & Zhong, P. (2019). Spectral optimization of color temperature tunable white LEDs with red LEDs instead of phosphor for an excellent IES color fidelity index. *OSA Continuum, 2*(4), 1056-1064.

[19] Zhao, B., Xu, Q., & Luo, M. R. (2020). Color difference evaluation for wide-color-gamut displays. *JOSA A, 37*(8), 1257-1265.

[20] Loan, N. T. P., & Le, A. T. (2020). Enhance the chromatic uniformity and luminous efficiency of WLEDs with triple-layer remote phosphor structures. *International Journal of Electrical and Computer Engineering (IJECE), 10*(6), 6244-6250.

[21] Loan, N. T. P., & Le, A. T. (2020). Enhance the chromatic uniformity and luminous efficiency of WLEDs with triple-layer remote phosphor structures. *International Journal of Electrical and Computer Engineering (IJECE), 10*(6), 6244-6250.

About Authors

Nguyen Hai Son DANG was born in Ho Chi Minh city, Vietnam. He has been studying at the Faculty of Electrical and Electronics Engineering, Ton Duc Thang University. His research interest is optoelectronics and lighting design. He has been working at Nam Viet technology & trading corporation.

Doan Minh Thong NGUYEN was born in Ho Chi Minh city, Vietnam. He has been studying at the Faculty of Electrical and Electronics Engineering, Ton Duc Thang University. He has been working at Nam Viet Technology & Trading corporation. His research interest is optoelectronics and lighting design.

Thi Phuong Loan NGUYEN was born in Da Nang province. In 2006, She received her master degree from University of Natural Sciences. Her research interest is optoelectronics. She has worked at the Faculty of Fundamental 2, Posts and Telecommunications Institute of Technology, Ho Chi Minh City, Vietnam.

Doan Quoc Anh NGUYEN was born in Khanh Hoa province, Vietnam. He has been working at the Faculty of Electrical and Electronics Engineering, Ton Duc Thang University. Quoc Anh received his PhD degree from National Kaohsiung University of Science and Technology, Taiwan in 2014. His research interest is optoelectronics.

Hsiao-Yi LEE was born in Hsinchu city, Taiwan. He has been working at the Department of Electrical Engineering, National Kaohsiung University of Science and Technology, Kaohsiung, Taiwan. His research interest is optics science.